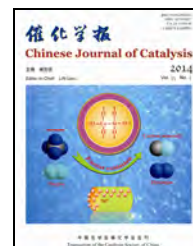




available at www.sciencedirect.com



journal homepage: www.elsevier.com/locate/chnjc



## Article

# Polyvinyl amine coated Fe<sub>3</sub>O<sub>4</sub>@SiO<sub>2</sub> magnetic microspheres for Knoevenagel condensation

Farzad Zamani <sup>a,b,\*</sup>, Elham Izadi <sup>a,b</sup><sup>a</sup> Department of Chemistry, Shahreza Branch, Islamic Azad University, Shahreza 31186145, Isfahan, Iran<sup>b</sup> Laboratory of Applied Chemistry, Central Laboratory Complex, Isfahan Science and Technology Town, Isfahan University of Technology, Isfahan 8415683111, Iran

## ARTICLE INFO

## Article history:

Received 20 July 2013

Accepted 16 August 2013

Published 20 January 2014

## Keywords:

Basic magnetic catalyst

Fe<sub>3</sub>O<sub>4</sub> nanoparticle

Polyvinyl amine

Knoevenagel condensation

## ABSTRACT

Polyvinyl amine coated Fe<sub>3</sub>O<sub>4</sub>@SiO<sub>2</sub> composite microspheres with a core-shell structure were prepared and employed as a magnetic catalyst for Knoevenagel condensation under mild conditions. The catalyst can be readily recovered using a magnet and reused several times without loss in activity or selectivity. The performance of the magnetic base catalyst was compared with that of polyvinyl amine functionalized mesoporous SBA-15, which showed that the magnetic nanoparticles gave improved reaction rate and yield.

© 2014, Dalian Institute of Chemical Physics, Chinese Academy of Sciences.

Published by Elsevier B.V. All rights reserved.

## 1. Introduction

In recent years, organic-inorganic hybrid materials that combine the properties of inorganic and organic components within a single material have attracted interest due to their advantages that a polymer matrix has facile processing, flexibility, and various functional groups and the inorganic component has mechanical and thermal stability as well as strength [1,2]. Organic-inorganic hybrid materials can have novel and excellent properties by the varying of their composition, dimension, and structure.

Magnetic nanoparticles (e.g. Fe<sub>3</sub>O<sub>4</sub>) have been investigated as inorganic supports for the synthesis of organic-inorganic hybrid materials because of their potential application in many industrial and biological fields [3]. Their magnetic property allows response to a magnet, making sampling and collection easier. Fe<sub>3</sub>O<sub>4</sub> nanoparticles are naturally hydrophilic because of the existence of plentiful hydroxyl groups on the particle sur-

face. Because they are prone to aggregation, their dispersion in an organic medium is difficult, and the surface coating or modification of iron oxide nanoparticles is very important in both academic and industrial fields. The formation of magnetite/polymer hybrid materials not only stabilizes the magnetic nanoparticles but also endows the magnetic nanoparticles with functionality, thus, magnetic polymer hybrid microspheres have been widely used in biology, medicine, and catalysis [4–8].

The Knoevenagel condensation of aldehydes with compounds containing activated methylene groups is one of the most useful and widely employed methods for carbon-carbon bond formation. It has numerous applications in the synthesis of fine chemicals and biological compounds [9,10]. Conventionally, this reaction is catalyzed by weak bases like primary, secondary, and tertiary amines under homogeneous conditions, which suffers from many drawbacks such as difficult catalyst recovery and low yield [11]. Over the last decade, various solid-supported catalysts and magnetite/polymer hybrid materi-

\* Corresponding author. Tel: +98-311-3865355; Fax: +98-311-3869714; E-mail: fzamani@iaush.ac.ir

DOI: 10.1016/S1872-2067(12)60685-8 | http://www.sciencedirect.com/science/journal/18722067 | Chin. J. Catal., Vol. 35, No. 1, January 2014

als have been applied to it in order to solve the main difficulties in this reaction [12–22].

In continuing our development of efficient and environmentally benign organic-inorganic solid catalysts [23–25], here we report the preparation of polyvinyl amine (PVAm)-coated  $\text{Fe}_3\text{O}_4@/\text{SiO}_2$  composite microspheres as a magnetically recoverable basic catalyst. The catalytic activity of this new magnetic basic catalyst was tested for Knoevenagel condensation under mild conditions. The catalytic performance of the magnetic was compared with that of polyvinyl amine-coated mesoporous SBA-15 [26].

## 2. Experimental

### 2.1. Catalyst preparation

The procedure for preparing PVAm-coated  $\text{Fe}_3\text{O}_4@/\text{SiO}_2$  composite microspheres has four steps. The schematic procedure is illustrated in Scheme 1. The detailed procedure is as follows.

In the first step,  $\text{Fe}_3\text{O}_4$  nanoparticles were synthesized by chemical co-precipitation [27].  $\text{FeCl}_3 \cdot 6\text{H}_2\text{O}$  (12.0 g) and  $\text{FeCl}_2 \cdot 4\text{H}_2\text{O}$  (4.90 g) were dissolved in 50 mL deionized water with mechanical stirring at 80 °C, followed by the addition of 80 mL ammonia (25 wt%, aqueous solution). The dispersion was stirred for 30 min upon addition of trisodium citrate (1.40 g). The resultant magnetite particles were separated with a magnet, washed several times with deionized water, and dried at 60 °C under vacuum for 24 h.

In the second step,  $\text{Fe}_3\text{O}_4@/\text{SiO}_2$  core-shell microspheres were prepared according to the Stöber method [28].  $\text{Fe}_3\text{O}_4$  (1 g), 4 mL of ammonia (25 wt%), and 20 mL of deionized water were mixed with 70 mL of ethanol. After ultrasonication for 10 min, 0.5 mL of tetraethyl orthosilicate (TEOS) was added to the mixture with continuous stirring. After reaction for more than 8 h, the product was collected by a magnet, washed several times with water and absolute ethanol. Finally, the product was dried in a vacuum oven at 60 °C for 24 h to yield  $\text{Fe}_3\text{O}_4@/\text{SiO}_2$ .

In the third step, surface modification of the magnetic  $\text{Fe}_3\text{O}_4@/\text{SiO}_2$  core-shell microspheres was carried out using the method reported in the literature [26].  $\text{Fe}_3\text{O}_4@/\text{SiO}_2$  (0.1 g) and acrylamide monomer (0.05 g) in THF (7 mL) were placed in a round bottom flask and sonicated for 10 min. Benzoyl peroxide (0.005 g) as initiator was then added, and the mixture was heated to 75 °C for 5 h while stirring. Finally, the resulting solid material was removed by a magnet and dried at 60 °C over-

night under vacuum to obtain  $\text{Fe}_3\text{O}_4@/\text{SiO}_2\text{-PAM}$ .

In the last step, in order to convert polyacryl amide to polyvinyl amine, Hofmann degradation was carried out with  $\text{Ca}(\text{OCl})_2$ .  $\text{Fe}_3\text{O}_4@/\text{SiO}_2\text{-PAM}$  (0.1 g), deionized water (10 mL), and  $\text{Ca}(\text{OCl})_2$  (0.08 g) were placed into a round bottom flask and sonicated for 10 min. The suspension was then refluxed for 6 h. Afterwards, it was separated using a magnet, washed with deionized water, and finally dried at 60 °C overnight under vacuum to yield polyvinyl amine-coated  $\text{Fe}_3\text{O}_4@/\text{SiO}_2$  ( $\text{Fe}_3\text{O}_4@/\text{SiO}_2\text{-PVAm}$ ).

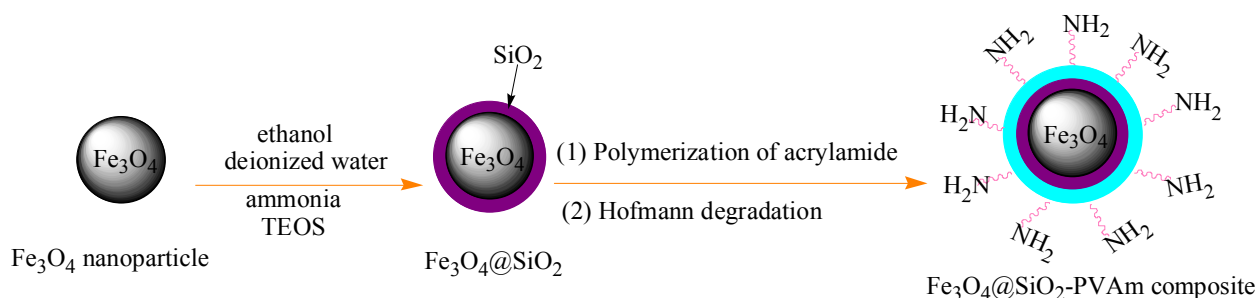
The basic site content of the  $\text{Fe}_3\text{O}_4@/\text{SiO}_2\text{-PVAm}$  composite was measured by back titration using NaOH. HCl (0.2 mol/L, 3 mL) was added to 0.02 g of the composite and stirred for 30 min. The catalyst was removed and washed successively with deionized water. The excess amount of HCl was titrated with NaOH (0.1 mol/L) using phenolphthalein as indicator. The amine content of catalyst was 9.24 mequiv/g.

### 2.2. Catalyst characterization

The crystalline structure of the samples was characterized by X-ray diffraction (XRD) analysis on a Bruker D8 Advance diffractometer with  $\text{Cu } K_\alpha$  radiation at 40 kV and 20 mA. Fourier transform infrared (FT-IR) spectra were recorded with a Perkin Elmer 65 spectrometer in the range of 400–4000  $\text{cm}^{-1}$ . Transmission electron microscopy (TEM) analysis was performed on a Phillips CM10 microscope at an accelerating voltage of 200 kV. Magnetization measurements were carried out on a BHV-55 vibrating sample magnetometer (VSM).

### 2.3. Knoevenagel condensation catalyzed by $\text{Fe}_3\text{O}_4@/\text{SiO}_2\text{-PVAm}$

In a typical reaction, a mixture of  $\text{Fe}_3\text{O}_4@/\text{SiO}_2\text{-PVAm}$  composite (0.05 g), benzaldehyde (1 mmol), and ethanol (5 mL) was placed in a round bottom flask. The reaction vessel was sonicated for 5 min at room temperature to disperse the magnetic nanoparticles in the solution. Then, ethyl cyanoacetate (1 mmol) was added to the mixture and stirred at room temperature for 30 min. The progress of the reaction was monitored by thin layer chromatography (TLC). After completion of the reaction, the catalyst was separated with a magnet and was washed with hot ethanol. Then, the solvent was evaporated. The products were identified using  $^1\text{H}$  NMR,  $^{13}\text{C}$  NMR, and FT-IR spectroscopy. Quantitative analyses were conducted with an Agilent 6820 gas chromatograph equipped with an FID detector.



**Scheme 1.** Schematic of the procedure for the preparation of  $\text{Fe}_3\text{O}_4@/\text{SiO}_2\text{-PVAm}$  composite microspheres with core-shell structure.

### 3. Results and discussion

#### 3.1. Catalyst characterization

The crystalline structure of the different synthesized materials was investigated by XRD. For the  $\text{Fe}_3\text{O}_4$  particles (Fig. 1(1)), the diffraction peaks at  $2\theta = 30.1^\circ, 35.4^\circ, 43.1^\circ, 53.4^\circ, 56.9^\circ,$  and  $62.5^\circ$  corresponded to the spinel structure of  $\text{Fe}_3\text{O}_4$  [29], which can be assigned to the diffraction of the (220), (311), (400), (422), (511), and (440) planes of the crystals, respectively. For the  $\text{Fe}_3\text{O}_4@SiO_2$  and  $\text{Fe}_3\text{O}_4@SiO_2\text{-PVAm}$  samples (Fig. 1(2) and (3)), the XRD patterns indicated that the crystalline structure of the  $\text{Fe}_3\text{O}_4$  particles was retained after the deposition of the polymer layers. The broad peak at around  $2\theta \approx 24^\circ$  indicated the presence of amorphous silica in  $\text{Fe}_3\text{O}_4@SiO_2$  (Fig. 1(2)). The intensity of this peak increased with the introducing of polyvinyl amine on the silica-coated magnetic nanoparticles (Fig. 1(3)), which can be attributed to the amorphous polymer supported on the composite [30]. The XRD results showed that the  $\text{Fe}_3\text{O}_4@SiO_2$  particles have been successfully coated with polyvinyl amine.

Figure 2 depicts the FT-IR spectra of the  $\text{Fe}_3\text{O}_4@SiO_2$ , PVAm, and  $\text{Fe}_3\text{O}_4@SiO_2\text{-PVAm}$  composites. An absorption peak at  $596\text{ cm}^{-1}$  is the characteristic absorption of a Fe–O bond, confirming the presence of  $\text{Fe}_3\text{O}_4$  nanoparticles. This was present in the spectra of  $\text{Fe}_3\text{O}_4@SiO_2$  and  $\text{Fe}_3\text{O}_4@SiO_2\text{-PVAm}$ . The adsorption peaks at  $1090$  and  $803\text{ cm}^{-1}$  corresponds to the asymmetric and symmetric stretching vibration of Si–O–Si bond in oxygen-silica tetrahedron, respectively, indicating that the  $\text{Fe}_3\text{O}_4$  microspheres were successfully coated with a  $SiO_2$  layer (Fig. 2(1) and (3)). For  $\text{Fe}_3\text{O}_4@SiO_2\text{-PVAm}$ , the new band located at  $1439\text{ cm}^{-1}$  can be attributed to the bending vibration absorption of the N–H bond [26]. In addition, the peak at  $3425\text{ cm}^{-1}$  was stronger than in the FT-IR spectrum of  $\text{Fe}_3\text{O}_4@SiO_2$ , showing the presence of the stretching vibration of the N–H groups in the structure of  $\text{Fe}_3\text{O}_4@SiO_2\text{-PVAm}$  [26]. The bands in the  $2800\text{--}3000\text{ cm}^{-1}$  region are attributed to the stretching of C–H bonds of the saturated alkane (Fig. 2(3)) [31], which were in agreement with the spectrum of PVAm. A closer examination of the spectrum of  $\text{Fe}_3\text{O}_4@SiO_2\text{-PVAm}$  showed that there was no

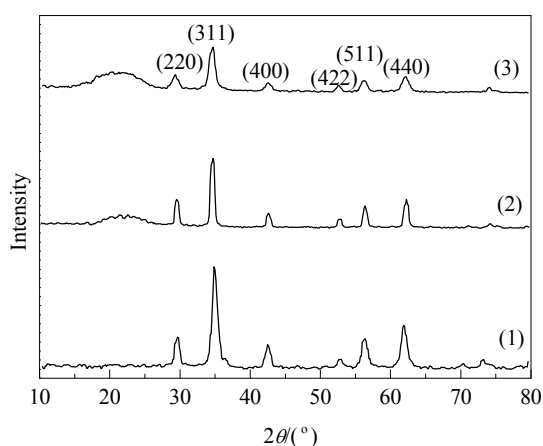


Fig. 1. XRD patterns of  $\text{Fe}_3\text{O}_4$  nanoparticles (1),  $\text{Fe}_3\text{O}_4@SiO_2$  (2), and  $\text{Fe}_3\text{O}_4@SiO_2\text{-PVAm}$  composite microspheres (3).

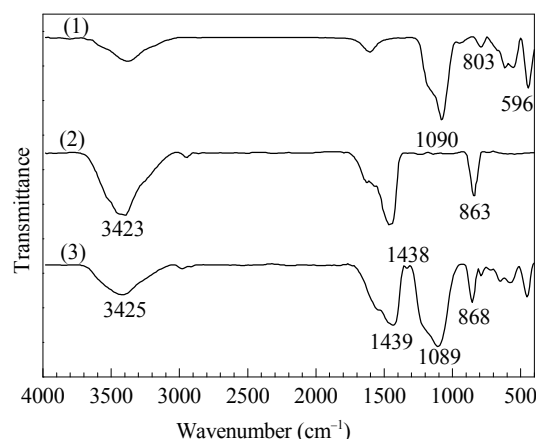


Fig. 2. FT-IR spectra of  $\text{Fe}_3\text{O}_4@SiO_2$  (1), PVAm (2), and  $\text{Fe}_3\text{O}_4@SiO_2\text{-PVAm}$  composite microspheres (3).

characteristic absorption peak of the carbonyl group ( $\text{C}=\text{O}$ ), which is located at around  $1625\text{ cm}^{-1}$ . This indicated that the amide groups in the composite have been converted to amine groups by the Hofmann degradation used. Thus, it was concluded that a  $\text{Fe}_3\text{O}_4@SiO_2\text{-PVAm}$  composite was obtained.

The morphology of the composite microspheres was observed by TEM. Figure 3 displays the TEM micrographs of the  $\text{Fe}_3\text{O}_4@SiO_2$  core-shell and  $\text{Fe}_3\text{O}_4@SiO_2\text{-PVAm}$  composite microspheres. In the case of  $\text{Fe}_3\text{O}_4@SiO_2$  (Fig. 3(a)), a continuous layer of  $SiO_2$  was clearly observed on the outer shell of the  $\text{Fe}_3\text{O}_4$  microsphere core, which had a diameter size of  $40\text{ nm}$ . After compositing with PVAm, a thin PVAm layer was deposited on the surface of the  $\text{Fe}_3\text{O}_4@SiO_2$  microspheres, and the particles were fully encapsulated by the PVAm polymer layer (Fig. 2(b)) to form a core-shell structure (Fig. 3(b)), with the size of  $250$  to  $300\text{ nm}$ . Furthermore, these composites still maintained their spherical shape after the coating of  $SiO_2$  and PVAm.

In order to investigate the influence of the PVAm polymer on the magnetic properties of  $\text{Fe}_3\text{O}_4@SiO_2$  core-shell microspheres, the magnetic properties of  $\text{Fe}_3\text{O}_4@SiO_2$  and  $\text{Fe}_3\text{O}_4@SiO_2\text{-PVAm}$  composites were measured by VSM. Typical magnetization curves of the samples with the applied magnetic field at room temperature are shown in Fig. 4. The absence of hysteresis for both samples indicated that the products have paramagnetism at room temperature. The magnetic saturation value reached  $61.4\text{ emu/g}$  for the  $\text{Fe}_3\text{O}_4$  nanoparticles coated with  $SiO_2$ . The magnetic saturation value decreased to  $45.2$

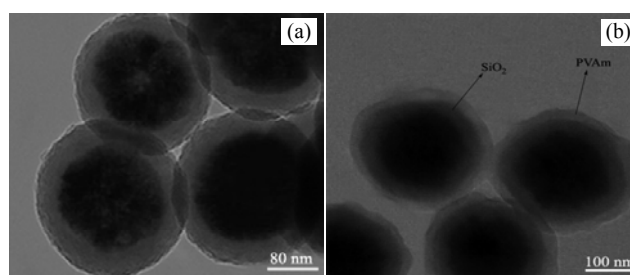
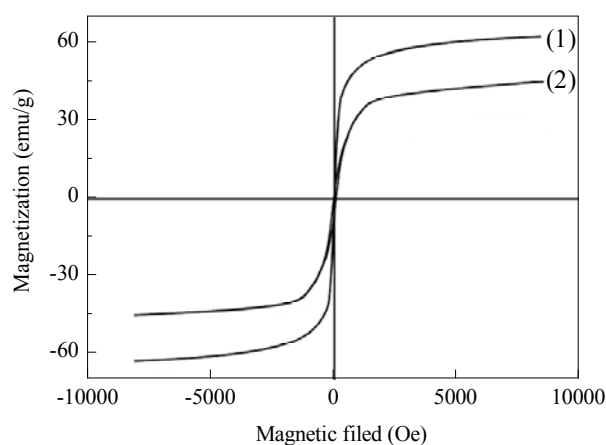


Fig. 3. TEM images of  $\text{Fe}_3\text{O}_4@SiO_2$  (a) and  $\text{Fe}_3\text{O}_4@SiO_2\text{-PVAm}$  composite microspheres (b).



**Fig. 4.** Room temperature magnetization curves of  $\text{Fe}_3\text{O}_4@SiO_2$  (1) and  $\text{Fe}_3\text{O}_4@SiO_2$ -PVAm composite microspheres (2).

emu/g for the  $\text{Fe}_3\text{O}_4@SiO_2$ -PVAm composite microspheres, which was possibly due to the non-magnetic polyvinyl amine coating. The magnetic properties and TEM analysis further proved the presence of a PVAm shell around the  $\text{Fe}_3\text{O}_4@SiO_2$  particles.

### 3.2. Catalytic activity

$\text{Fe}_3\text{O}_4@SiO_2$ -PVAm as a solid basic catalyst for C–C bond formation in Knoevenagel condensation was evaluated. A model reaction for benzaldehyde and ethyl cyanoacetate as the substrates in Knoevenagel condensation was investigated over the catalyst at room temperature to optimize the reaction conditions and to obtain the best catalytic activity. Ethanol was chosen as the best solvent for the Knoevenagel condensation according to a previous work [26].

In order to find the maximum amount of PVAm functionalized on the surface of  $\text{Fe}_3\text{O}_4@SiO_2$ , catalysts with different ratios of  $\text{Fe}_3\text{O}_4@SiO_2$  (0.1 g) to PVAm (0–0.5 g) were prepared, and their catalytic activity was tested for Knoevenagel condensation (Table 1). It can be seen that as the ratio of  $\text{Fe}_3\text{O}_4@SiO_2$ -PVAm increased, the reaction yield increased. The probable reason is that when the amount of  $\text{Fe}_3\text{O}_4@SiO_2$  increased, the polymeric material gets more ordered on the surface of the magnetic microspheres [26]. Therefore, the functional groups of the polymer were more exposed and more effective. From the results, the best mass ratio of  $\text{Fe}_3\text{O}_4@SiO_2$  to

**Table 1**

Effect of the  $\text{Fe}_3\text{O}_4@SiO_2$  to PVAm ratio on catalytic activity of  $\text{Fe}_3\text{O}_4@SiO_2$ -PVAm.

$\text{Fe}_3\text{O}_4@SiO_2$ /PVAm mass ratio	Isolated yield (%)
3.5	38
3.0	55
2.5	69
2.0	48
Without PVAm	4 <sup>a</sup>

Reaction conditions: benzaldehyde 1 mmol, ethyl cyanoacetate 1 mmol, catalyst 0.03 g, ethanol 5 mL, reaction time 30 min (<sup>a</sup> 4 h), room temperature, selectivity 100%.

**Table 2**

Effect of catalyst amount on the Knoevenagel condensation.

Amount of catalyst (g)	Isolated yield (%)
0.03	69
0.04	82
0.05	95
0.06	95

Reaction conditions: benzaldehyde 1 mmol, ethyl cyanoacetate 1 mmol, reaction time 30 min, room temperature, selectivity 100%.

acryl amide was 2.5 for these components. It should be noted that the non-functionalized magnetic nanoparticles ( $\text{Fe}_3\text{O}_4@SiO_2$ ) were not active in the Knoevenagel condensation, with less than 5% conversion observed after 4 h. This indicated the need for the polymer coating on the surface of the magnetic nanoparticles to create basic sites.

To study the effect of catalyst amount, the Knoevenagel condensation was carried out with different amounts of catalyst (Table 2). When the amount of catalyst increased from 0.03 to 0.05 g, the product yield increased significantly from 69% to 95%, which was due to the availability of more basic sites. After that, the yield remained almost stable between 0.05 g and 0.06 g. Therefore, 0.05 g was chosen as the optimized amount of catalyst for further experiments.

In addition, in order to investigate the importance of the support ( $\text{Fe}_3\text{O}_4@SiO_2$ ), the Knoevenagel condensation of benzaldehyde and ethyl cyanoacetate over PVAm was examined under optimum reaction conditions. A yield of 38% was observed after 2 h. This showed that the existence of the support ( $\text{Fe}_3\text{O}_4@SiO_2$ ) in this magnetic composite played a critical role in the efficiency of the catalyst.

The activity of  $\text{Fe}_3\text{O}_4@SiO_2$ -PVAm for Knoevenagel condensation reaction was determined using ethyl cyanoacetate, diethyl malonate, and acetoacetic ester as active methylene reagents (Table 3). It was observed that ethyl cyanoacetate ( $pK_a \approx 9$ ) and acetoacetic ester ( $pK_a \approx 11$ ) can be deprotonated by the catalyst to generate the corresponding carbanion, followed by attack on the electron acceptor center. Moreover, it was found that the catalyst was not able to pull off protons from diethyl malonate ( $pK_a \approx 13$ ) and the Knoevenagel adducts with this substrate were not obtained. This observation showed that the catalyst has surface basic sites with  $pK_a$  lower than 13. The highest benzaldehyde yield (95%) was obtained using ethyl cyanoacetate.

In general, when using a supported catalyst, a crucial issue is the possibility that some active sites are lost from the solid support to the liquid phase, and these leached species are responsible for a significant loss of the catalytic activity. There-

**Table 3**

Effect of active methylene reagents on the Knoevenagel condensation over  $\text{Fe}_3\text{O}_4@SiO_2$ -PVAm.

Active methylene reagent	Time (min)	Isolated yield (%)
Ethyl cyanoacetate	30	95
Diethyl malonate	360	—
Acetoacetic ester	30	42

Reaction conditions: benzaldehyde 1 mmol, catalyst 0.05 g, active methylene reagent 1 mmol, reaction time 30 min, room temperature, 100% selectivity.

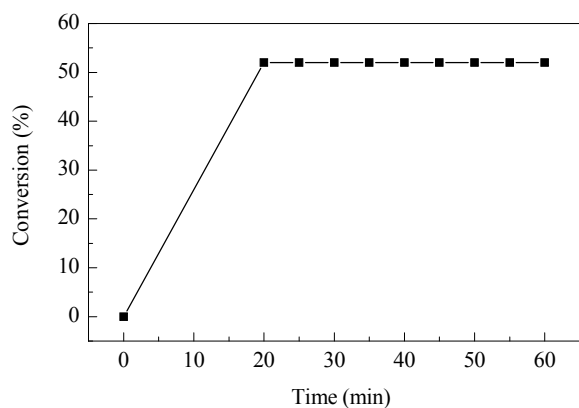


Fig. 5. Heterogeneity test for Knoevenagel condensation of benzaldehyde with ethyl cyanoacetate.

fore, in order to prove the heterogeneous nature of the catalyst, a heterogeneity test was performed, in which the catalyst was separated from the reaction mixture at approximately 50% conversion of the starting material by a magnet. The reaction progress in the filtrate was monitored (Fig. 5). No further reaction conversion was observed even at extended time, indicating that the nature of reaction process was heterogeneous and there was no reaction in the homogeneous phase.

For use for industrial purposes, reusability of the catalyst was tested by carrying out repeated runs of the reaction with the same batch of the catalyst with the model reaction (Fig. 6). In order to regenerate the catalyst after each cycle, it was separated by a permanent magnet and washed several times with deionized water and ethanol. Then, it was dried in an oven at 60 °C and used in the Knoevenagel condensation. The results showed that this catalyst can be reused ten times without significant loss of activity or selectivity in the Knoevenagel condensation.

The  $\text{Fe}_3\text{O}_4@\text{SiO}_2\text{-PVAm}$  catalyst also gave good activity and selectivity in the Knoevenagel condensation of different kinds of aromatic and aliphatic aldehydes and ethyl cyanoacetate (Table 4). All the investigated reactions were almost completed in 10–45 min and produced the corresponding alkenes in high yield without the formation of any side product.

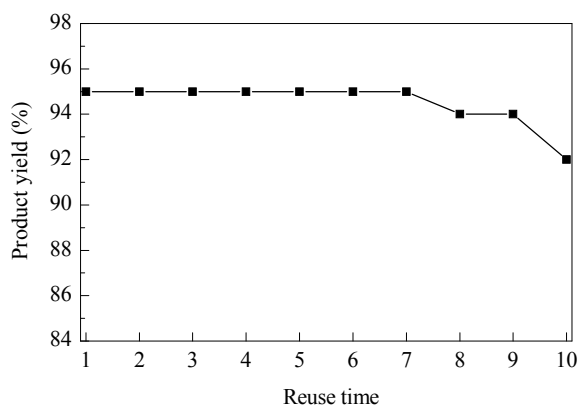


Fig. 6. Recyclability of the catalyst. Reaction conditions: benzaldehyde 1 mmol, ethyl cyanoacetate 1 mmol, catalyst 0.05 g, reaction time 30 min, room temperature, 100% selectivity.

Table 4

Knoevenagel condensation of various aromatic and aliphatic aldehydes and ethyl cyanoacetate catalyzed by  $\text{Fe}_3\text{O}_4@\text{SiO}_2\text{-PVAm}$ .

Entry	Substrate	Product	Time (min)	Isolated yield (%)
1			30	95
2			10	95
3			45	78
4			20	86
5			20	95
6			10	98
7			10	98
8			20	45
9			45	87 <sup>a</sup>
10			40	90 <sup>a</sup>

Reaction conditions: substrate 1 mmol, ethyl cyanoacetate 1 mmol, catalyst 0.05 g, ethanol 5 mL, room temperature, 100% selectivity.

<sup>a</sup> GC yield.

The catalytic activity of  $\text{Fe}_3\text{O}_4@\text{SiO}_2\text{-PVAm}$  in Knoevenagel condensation was compared with that of the SBA-15/PVAm composite reported in the literature [26]. The results are summarized in Table 5. As can be seen,  $\text{Fe}_3\text{O}_4@\text{SiO}_2\text{-PVAm}$  gave a higher activity in Knoevenagel condensation at a shorter time and under a milder condition (room temperature) compared to SBA-15/PVAm.

In general, when porous inorganic materials are used as support, a substantial decrease in activity of the immobilized catalyst is commonly observed, especially in a liquid phase reaction, due to the problem of slow reactant diffusion to the catalyst anchored on the interior surface [32]. In contrast, nanoparticles, especially magnetic nanoparticles, are more efficient support materials for homogeneous catalyst immobiliza-

**Table 5**Comparison of the catalytic activity of Fe<sub>3</sub>O<sub>4</sub>@SiO<sub>2</sub>-PVAm and SBA-15/PVAm in Knoevenagel condensation.

Catalyst	Time (min)	Temperature	Yield (%)	Ref.
Fe <sub>3</sub> O <sub>4</sub> @SiO <sub>2</sub> -PVAm magnetic microspheres <sup>a</sup>	30	room temperature	95 <sup>c</sup>	this work
SBA-15/PVAm mesoporous composite <sup>b</sup>	120	78 °C (reflux)	90 <sup>d</sup>	[26]

<sup>a</sup> Reaction conditions: benzaldehyde 1 mmol, ethyl cyanoacetate 1 mmol, catalyst 0.05 g, ethanol 5 mL.<sup>b</sup> Reaction conditions: benzaldehyde 2 mmol, ethyl cyanoacetate 2 mmol, catalyst 0.12 g, ethanol 10 mL.<sup>c</sup> Isolated yield.<sup>d</sup> GC yield.

tion [33]. When nonporous nanoparticles are used as the support, the size of the support materials is decreased to the nanometer scale, and all the catalytic sites are on the external surface of the particles and are accessible to the substrates. As a consequence, the activity of nanoparticle-supported catalysts is improved compared to homogeneous catalysts immobilized on conventional porous supports, where internal pore diffusion in the porous catalysts can be rate limiting. This would explain the higher activity at a shorter time and milder condition for the catalyst here (Fe<sub>3</sub>O<sub>4</sub>@SiO<sub>2</sub>-PVAm) compared to SBA-15/PVAm.

#### 4. Conclusions

A facile route for the synthesis of polyvinyl amine coated Fe<sub>3</sub>O<sub>4</sub>@SiO<sub>2</sub> composite microspheres was demonstrated. This new basic magnetic catalyst is better than soluble bases because it has the following advantages: (a) high catalytic activity in Knoevenagel condensation under mild reaction conditions; (b) easy separation after the reaction by a magnet; (c) simple catalyst preparation; and (d) reusable several times without loss of activity or selectivity. In addition, the basic magnetic catalyst is a better alternative to amino-functionalized porous silica catalysts for Knoevenagel condensation because its catalytic sites are more accessible than those in the porous silica materials.

#### Acknowledgments

The authors thank Isfahan Science and Technology Town (Isfahan University of Technology) for the support of this work.

#### References

- [1] Sanchez C, Soler-Illia G J A A, Ribot F, Lalot T, Mayer C R, Cabuil V. *Chem Mater*, 2001, 13: 3061
- [2] Hoffmann F, Cornelius M, Morell J, Fröba M. *Angew Chem Int Ed*, 2006, 45: 3216
- [3] Kumar K S, Kumar V B, Paik P. *J Nanoparticles*, 2013, Article ID 672059, 24 pages
- [4] Rana S, White P, Bradley M. *Tetrahedron Lett*, 1999, 40: 8137
- [5] Liu X Q, Guan Y P, Ma Z Y, Liu H Z. *Langmuir*, 2004, 20: 10278
- [6] Kara A, Erdem B. *J Mol Catal A*, 2011, 349: 42
- [7] Kawashita M, Tanaka M, Kokubo T, Inoue Y, Yao T, Hamada S, Shinjo T. *Biomaterials*, 2005, 26: 2231
- [8] Deng Y H, Wang C C, Shen X Z, Yang W L, Jin L, Gao H, Fu S K. *Chem Eur J*, 2005, 11: 6006
- [9] Freeman F. *Chem Rev*, 1980, 80: 329
- [10] Tietze L F. *Chem Rev*, 1996, 96: 115
- [11] Jackson D B, Macquarrie D J, Clark J H. In: Sherrington D C, Kybett A P Eds. *Supported Catalysts and their Applications*. Cambridge: Royal Society of Chemistry, 2001. 203
- [12] Kim K S, Song J H, Kim J H, Seo G. *Stud Surf Sci Catal*, 2003, 146: 505
- [13] Yamashita K, Tanaka T, Hayashi M. *Tetrahedron*, 2005, 61: 7981
- [14] Phan N T S, Jones C W. *J Mol Catal A*, 2006, 253: 123
- [15] Karaoglu E, Baykal A, Senel M, Sözeri H, Toprak M S. *Mater Res Bull*, 2012, 47: 2480
- [16] Chen X Q, Arruebo M, Yeung K L. *Catal Today*, 2013, 204: 140
- [17] Zhang Y, Xia C G. *Appl Catal A*, 2009, 366: 141
- [18] Parida K M, Mallick S, Sahoo P C, Rana S K. *Appl Catal A*, 2010, 381: 226
- [19] Nemati F, Heravi M M, Saedirad R. *Chin J Catal* (催化学报), 2012, 33: 1825
- [20] Rostami A, Atashkar B, Gholami H. *Catal Commun*, 2013, 37: 69

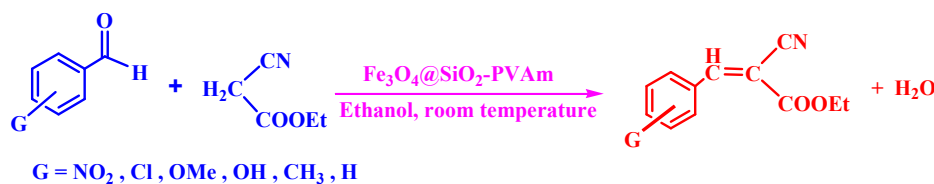
#### Graphical Abstract

*Chin. J. Catal.*, 2014, 35: 21–27 doi: 10.1016/S1872-2067(12)60685-8

#### Polyvinyl amine coated Fe<sub>3</sub>O<sub>4</sub>@SiO<sub>2</sub> magnetic microspheres for Knoevenagel condensation

Farzad Zamani\*, Elham Izadi

Islamic Azad University, Iran; Isfahan University of Technology, Iran



Polyvinyl amine coated Fe<sub>3</sub>O<sub>4</sub>@SiO<sub>2</sub> was prepared by a simple method. This new magnetic catalyst exhibited high catalytic activity in Knoevenagel condensation of various aromatic and aliphatic aldehydes under mild conditions along with excellent level of reusability.

- [21] Sharma R K, Monga Y, Puri A. *Catal Commun*, 2013, 35: 110
- [22] Shaterian H R, Aghakhanizadeh M. *Catal Sci Technol*, 2013, 3: 425
- [23] Kalbasi R J, Kolahdoozan M, Shahabian K, Zamani F. *Catal Commun*, 2010, 11: 1109
- [24] Kalbasi R J, Massah A R, Zamani F, Bain A D, Berno B. *J Porous Mater*, 2011, 18: 475
- [25] Kalbasi R J, Izadi E. *CR Chim*, 2011, 14: 1002
- [26] Kalbasi R J, Kolahdoozan M, Rezaei M. *Mater Chem Phys*, 2011, 125: 784
- [27] Liu G Y, Wang H, Yang X L, Li L Y. *Eur Polym J*, 2009, 45: 2023
- [28] Stöber W, Fink A, Bohn E. *J Colloid Interface Sci*, 1968, 26: 62
- [29] Cabrera L, Gutierrez S, Morales M P, Menendez N, Herrasti P. *J Magn Magn Mater*, 2009, 321: 2115
- [30] Deng H J, Lei Z L. *Composites B*, 2013, 54: 194
- [31] Chen Y, Qian Z, Zhang Z C. *Colloid Surf A*, 2008, 312: 209
- [32] Panster P, Wieland S. In: Cornils B, Herrmann W A Eds. *Applied Homogeneous Catalysis with Organometallic Compounds*. Weinheim: Wiley/VCH, 1996. Vol. 2. Chapter 3.1.1.3
- [33] Astruc D, Lu F, Aranzas J R. *Angew Chem Int Ed*, 2005, 44: 7852